Proceedings of the International Conference on Heat Exchanger Fouling and Cleaning - 2024 (Peer-reviewed)
April 21–26, 2024, Lisbon, Portugal; Editors: H.U. Zettler and E.M. Ishiyama

LOCAL THERMAL RESISTANCE MEASUREMENT DEVICE FOR FOULING DETECTION

Q.T. Pham, F. Ducros, Z. Anxionnaz-Minvielle*
Univ. Grenoble Alpes, CEA, LITEN, F-38000, Grenoble, France

ABSTRACT

Heat exchanger (HX) fouling is one of the main reason for heat recovery loss of efficiency and fouling detection can help to schedule maintenance operation and to optimize resource consumption. This works presents a patented fouling detection probe (FDP) based on the measurement of the related induced thermal resistance thanks to an electrically heated resistance temperature device. The main features of the device are presented, as well as the measurement protocol. A 1D device model is proposed to handle the corresponding use conditions and limitations. An example of a fouling situation from the food industry is described and the related potential FDP use is discussed. The thermal resistances (convection and fouling) measured with the FDP are consistent with both the 1D-model prediction and the literature data which is the first validation step of the FDP concept. Future works will then focus on a 2D-model development to take into account the 2D heat flux and the related experimental validation with well-known fluids.

INTRODUCTION

HXs are one of the key components of the energy efficiency strategies, since they enable heat energy recovery and transfer. However, their performances may be hindered by fouling, which leads to around 1 - 2.5% of global CO_2 emissions [1]. Heat exchanger fouling may lead to high pressure drop, reduction in cross sectional flow area (up to blockage), as well as temperature decrease and/or additional power consumption. It may even cause a loss of production if the product cannot be processed. It also may affect the product quality (in the case of food applications) and lead to possible bacterial contamination (biofilms) [2], [3]. In some applications, cleaning is expensive and up to 42% of the production time can be dedicated to the process cleaning [3]. As a consequence, in the food industry, HXs are cleaned daily, or more, whereas petrochemical applications may require a cleaning once or twice a year. Some authors have evaluated the costs of fouling and related cleaning up to 80% of the production costs [[2]]. Moreover, cleaning can account for as much as 50% of the water use (especially for agro-food processes)[4].

In general, whatever the application (dairy products, district heating, petrochemistry, etc.) the detection and monitoring of fouling over time is made with global measurements of pressure drop, flowrate and temperature (to assess heat transfer coefficients and fouling resistance)[5], [6], [7]. Sometimes HXs are also opened to visualize fouling deposits.

In addition to global measurements, fouling sensors based on temperature [8], [9], electrical [10] or acoustic parameters [11] exist [12]. Chen at al. [13] proposed a non-invasive lab-scale fouling probe in which the measurement principle is based on electrical resistance. This sensor is efficient, in particular for soft deposits (dairy products applications) but further developments are required in order to be used for production-scale applications. Simeone et al.[14] also developed a lab-scale system but based on optical measurements (fluorosensing). They demonstrated its suitability for enhancing clean-in-place monitoring but there is a need for future development prior to production-scale applications. Hooper et al. [15] managed to measure very thin fouling layers (± 20 µm) with an in-situ fluid dynamic gauging technique. Efficient but invasive sensors based on temperature difference measurement [16], [17] and piezo electrical effect (quartz crystal sensor) [18] have also been studied.

Such monitoring and non-invasive techniques are required in order to monitor the fouling-cleaning cycle so that the processes can be optimized, improving productivity and sustainability [19]. The current work presents a patented fouling detection technology based on the measurement of its induced thermal resistance as a result of the rise in temperature of a probe (ΔT_p) that is electrically heated [8], [20], [21]. The concept and working principles of the mentioned FDP are reported, together with the related uncertainties. Both the targeted use conditions and the physical constraints that come along with the device use will also be discussed. A 1D model is then derived, which establishes a relation between the induced

ISBN: 978-0-9984188-3-4; Published online www.heatexchanger-fouling.com

temperature difference ΔT_p measured by the FDP and the thermal fouling resistance. It also helps to determine the fouling resistance ranges that can be measured. An experimental case is presented and used to validate the model prediction.

TECHNOLOGICAL FEATURES OF THE FDP

The two patents [20], [21] describe some of the technological features of the FDP considered in this paper. The principle relies on the use of a resistance temperature device (RTD) in which the electrical resistance changes as a function of its temperature. The RTD wire is a pure material, typically platinum (Pt), nickel (Ni), or copper (Cu). The most popular RTD are the Pt100 sensors (with resistance of 100 Ω at 0°C). They have been used for many years to measure temperature in laboratory and industrial processes, and have developed a reputation for accuracy, repeatability, and stability. Other technologies, such asPt20 and Pt500 are also available. All these devices show a quasi-linear temperature dependence:

$$R_\Omega(T) = R_{\Omega,0}\big(1 + \alpha(T - T_0)\big) \quad (1)$$

in which $R_{\Omega,0}$ (Ω) stands for electrical resistance at reference temperature T_0 $(°C)$ and $R_\Omega(T)$ denotes the electrical resistance at a given temperature T (°C). Representative values for α are $6.41{\cdot}10^{-3}$, $3.93{\cdot}10^{-3}$ and $3.85{\cdot}10^{-3}$ $\Omega{\cdot}°C^{-1}$ for nickel, copper, and platinum, respectively.

The FDP developed at CEA (Fig. 1) consists of a thin layer resistor deposited between two dielectric films. The resistor is made of Nickel. The FDP is glued to the surface of the tube in which the working fluid circulates and through which the heat transfer occurs.

The FDP is supplied with direct current by a current generator. There are four wires, two for the current supply and the other two for measuring the voltage across the resistor terminals.

The measurement by the FDP is simultaneous with the two following steps:

- Step 1: Dissipate thermal power in the nickel thermo-sensitive resistor by the Joule effect. In that case, the FDP is used as a heat sink,
- Step 2: Measure the current and the voltage across the resistor in order to determine the resistance and therefore the equilibrium temperature of the probe as well as the power dissipated in the probe. This response depends on the thermal balance of the probe. It varies as a function of the thermal environment of the probe and therefore depends on the thickness of a possible fouling deposit if there are no external flow perturbations. Indeed, to identify a possible resistance due to fouling, the other thermal resistances and especially the one due to convection must remain constant.

The electronic device is a direct current generator capable of supplying one or more FDPs, measuring the supplied current and measuring the voltage across the FDP terminals. It is supplied with 220 V, 50 Hz and delivers a maximal power of 48 W. It is configured to operate the various measurements sequences without external intervention.

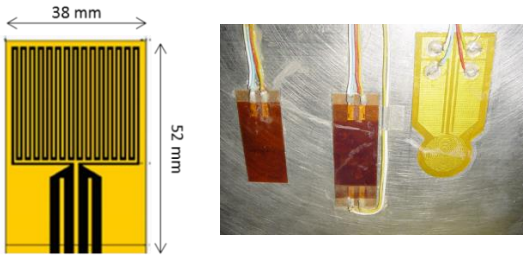

Fig. 1. FDP resistive circuit as developed at CEA (right) and as depicted in [20] (left) with the dielectric substrate (orange) and the Ni electric circuit (black). The four large tracks aim at both supplying the electric power and measuring the voltage.

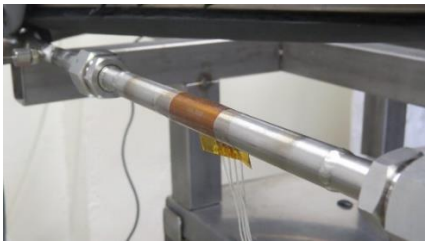

Fig. 2. RTD on a circular pipe in a situation that mimics an industrial process.

Fig. 2 illustrates a heat transfer situation in which fouling develops on the inner wall of the tube. This image shows that the probe size is small compared to the whole device. This means that the measured thermal resistance is local and depends on the FDP location. Also, the FDP geometry may be arbitrarily complex to fit the design of the equipment in which fouling occurs (corrugation of a plate-type heat exchanger for instance, not illustrated here).

EXPERIMENTAL SETUP AND PROCEDURE

The test rig dedicated to the fouling measurements and FDP characterization reproduces Ultra-High Temperature (UHT) treatment for cheese-like fluid. The flow diagram is illustrated in Fig. 3.

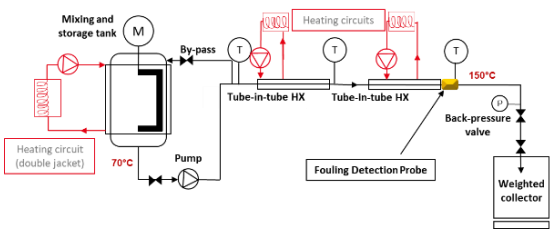

Fig. 3. Flow diagram of the experimental setup.

The fluid is pre-heated in a mixing tank from 6°C (storage temperature) to 70°C. Then it flows in

ISBN: 978-0-9984188-3-4; Published online www.heatexchanger-fouling.com

two tube-in-tube heat exchangers up to 150°C. The FDP is connected to the flow-type holder at the heat exchanger outlet (see Figs. 2 and 3). The holder is 300 mm long and its inner diameter is 10 mm. To avoid water vaporization during thermal treatment, the pressure is maintained at 4.5 bars with a back-pressure valve. The outlet temperature of the product is used as a process control input to the heating medium. Each test is calibrated to have a 2 h UHT process at steady state. The objective is to measure the fouling layer development with the FDP.

Then, following the thermal treatment step, a cleaning procedure is applied. In that case, the FDP is used to measure the cleaning efficiency (fouling layer removal). Several cleaning steps are involved but this article only focuses on the first step. This consists in rinsing the test rig and removing the cheese-like fluid with water at 80°C rather than to start cleaning the test section. It is referred to as flushing.

The test rig is equipped with Pt100 temperature sensors, electromagnetic flowmeter, absolute and differential pressure sensors and the FDP.

The operating conditions are summarized in the following Table 1.

Table 1. Operating conditions of the fouling and cleaning tests.

	Fouling step	Flushing step
Fluid	Cheese-like	Water
Temperature	150°C	80°C
Pressure	4.5 bars	1 bar
Flowrate	20 kg·h^{-1}	60 kg·h^{-1}
Reynolds number	3 500	6 060

In practice, at steady state (when the variation of the mean values of flowrate and temperature over a moving window is less than the standard deviation), the electrical resistance, R_Ω (Ω), of the FDP is measured for several steps of supplied power, P (W).

For each step of supplied power, the electrical resistance of the FDP stabilizes when the temperature equilibrium is reached. This value of R_Ω (Ω) is then measured and can be displayed on a graph as a function of P (W) for one measurement sequence (a sequence is made of several power steps). One measurement sequence is illustrated in Fig. 4. The slope of this curve, dR_Ω/dP (Ω·W^{-1}), is the useful information which is referred to as the FDP signal.

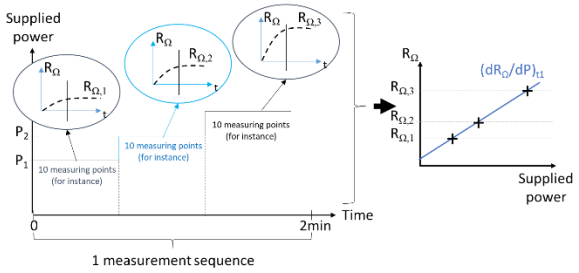

Fig. 4. Sketch of the measurement principle of the FDP.

During a fouling or a cleaning test, several measurement sequences are applied over time which allows plotting the FDP signal response vs. time, $dR_\Omega/dP=f(t)$ (see Fig.7 for example). This curve allows to monitor the fouling layer development over time assuming that the other thermal resistances have been maintained constant during the measurement campaign (no flow perturbation for instance that might affect the resistance due to convection).

1D MODELING

In this section, a 1D model is developed in order to evaluate the local thickness of fouling deposit on the inner wall of a heat exchanger by using the above presented FDP. As shown in Fig. 5, the FDP with dimension x_p (m), y_p (m), z_p (m) is located at the outer wall of the heat exchanger. A fluid flows into the heat exchanger in the x-direction with a given flow rate $\dot{m}$ (kg·s^{-1}). Under certain conditions, a fouling deposit starts developing at the inner wall of the heat exchanger. The thickness of this fouling deposit layer is designated as y_f (m). A uniform heat flux, φ_0 (W·m^{-2}), is applied along the y-axis to the surface of the FDP in Fig. 5.

For the 1D model, the following hypotheses are made:

- The heat flux applied to the FDP is assumed to pass through the wall of the heat exchanger as well as through the thickness of the fouling deposit in the y direction. The heat flux flows to the x and z directions are neglected. This is a major assumption that is planned to be addressed in our future works (see conclusion section).
- The dimensions of heat exchanger wall are x_w (m), y_w (m), z_w (m). They are assumed to be much larger than those of the FDP.
- The fouling thickness y_f (m) is supposed to be uniform under the cross-sectional area $S_p = x_p * z_p$ (m^2) of the FDP

The thermal conductivity of the fouling deposit λ_f (W·m^{-1}·K^{-1}) is considered constant across the area of the FDP.

ISBN: 978-0-9984188-3-4; Published online www.heatexchanger-fouling.com

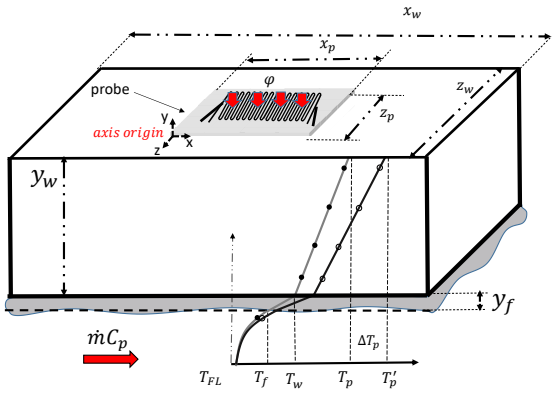

Fig. 5. Sketch of the current study FDP.

and Taking into account the above assumptions, the heat conduction in the solid parts is described as:

$$\boldsymbol{T_p - T_w = \varphi_0 \frac{y_w}{\lambda_w}} \quad (2)$$

$$\boldsymbol{T_w - T_f = \varphi_0 \frac{y_f}{\lambda_f}} \quad (3)$$

in which T_p (°C), T_w (°C), T_f (°C) are respectively denoted for probe temperature, wall temperature and fouling temperature.

These result in:

$$\boldsymbol{T_p - T_f = \varphi_0 \left(\frac{y_w}{\lambda_w} + \frac{y_f}{\lambda_f}\right)} \quad (4)$$

At the fouling/fluid interface, heat convection occurs with a heat transfer coefficient h (W·m^{-2}·K^{-1}), leading to:

$$\boldsymbol{T_f - T_{FL} = \frac{\varphi_0}{h}} \quad (5)$$

in which T_{FL} (°C) is the fluid temperature.

Combining the equations (4) and (5) reveals:

$$\boldsymbol{T_p - T_{FL} = \varphi_0 \left(\frac{y_w}{\lambda_w} + \frac{y_f}{\lambda_f} + \frac{1}{h}\right)} \quad (6)$$

The energy balance in the fluid part in the x-direction is written as:

$$\boldsymbol{\dot{m}Cp[T_{FL}(x) - T_{FL}(x=0)] = \varphi_0 x z_p} \quad (7)$$

in which $x = 0$ (left hand side edge of the FDP) to x_p andC_p (J·kg^{-1}·K^{-1}) is the heat capacity of the working fluid.

In case a heat flux $\varphi_0+\Delta\varphi$ (W·m^{-2}) is applied to the probe, then, with similar manipulations of the energy balance in the solid and fluid parts, the following equations are obtained as:

$$\boldsymbol{T'_p - T'_{FL} = (\varphi_0 + \Delta\varphi)\left(\frac{y_w}{\lambda_w} + \frac{y_f}{\lambda_f} + \frac{1}{h}\right)} \quad (8)$$

$$\boldsymbol{\dot{m}Cp[T'_{FL}(x) - T'_{FL}(x=0)] = (\varphi_0 + \Delta\varphi) x z_p} \quad (9)$$

wherein T'_p (°C) and T'_{FL} (°C) are the corresponding probe temperature and the fluid temperature. $T'_{FL}(x=0) = T_{FL}(x=0)$is the inlet fluid temperature. Combining the equations (7) and (9) gives:

$$\boldsymbol{\dot{m}Cp[T'_{FL}(x) - T_{FL}(x)] = \Delta\varphi x z_p} \quad (10)$$

Hence,

$$\boldsymbol{\Delta T_{FL}(x) = \frac{\Delta\varphi x z_p}{\dot{m}Cp}} \quad (11)$$

with: $\Delta T_{FL}(x) = T'_{FL}(x) - T_{FL}(x)$

Along the x-direction, the average fluid temperature can be written as:

$$\boldsymbol{\overline{T_{FL}} = \frac{T_{FL}(x_p) + T_{FL}(0)}{2}} \quad (12)$$

$$\boldsymbol{\overline{T'_{FL}} = \frac{T'_{FL}(x_p) + T_{FL}(0)}{2}} \quad (13)$$

in which $T_{FL}(x_p)$ (°C) and $T'_{FL}(x_p)$ (°C) are the fluid temperatures at $x = x_p$ when heat flux φ_0 and $\varphi_0+\Delta\varphi$ are applied to the FDP surface.

Then the difference of average fluid temperature for the two cases with application of heat flux φ_0 and $\varphi_0+\Delta\varphi$ becomes:

$$\boldsymbol{\overline{\Delta T_{FL}} = \frac{\Delta T_{FL}(x_p)}{2} = \frac{\Delta\varphi x_p z_p}{2\dot{m}Cp} = \frac{\Delta\varphi S_p}{2\dot{m}Cp}} \quad (14)$$

Using equations (7) and (9) for $x = x_p$ gives:

$$\boldsymbol{\Delta T_p(y_f) = T'_p - T_p} \quad (15)$$

$$\boldsymbol{= \Delta\varphi\left(\frac{y_w}{\lambda_w} + \frac{y_f}{\lambda_f} + \frac{1}{h}\right) + \overline{\Delta T_{FL}}}$$

For the case when $y_f = 0$ (no fouling), equation (15) becomes:

$$\boldsymbol{\Delta T_p(y_f = 0) = \Delta\varphi\left(\frac{y_w}{\lambda_w} + \frac{1}{h}\right) + \overline{\Delta T_{FL}}} \quad (16)$$

it allows the fouling deposit thickness to be determined as:

ISBN: 978-0-9984188-3-4; Published online www.heatexchanger-fouling.com

$$\frac{\boldsymbol{y_f}}{\boldsymbol{\lambda_f}} = \frac{\boldsymbol{\Delta T_p(y_f) - \Delta T_p(y_f = 0)}}{\boldsymbol{\Delta \varphi}} \quad (17)$$

in which, $\Delta T_p(y_f)$ (°C) and $\Delta T_p(y_f=0)$ (°C) are the induced temperature differences of the FDP.

Equation (17) allows determining the thickness of the fouling deposit for a given induced temperature measured by the FDP.

It is noted that in order to be exploitable, the fouling thickness should be greater than a threshold value. In the current study, a condition for the thermal resistance of the fouling deposit is defined as:

$$\frac{\boldsymbol{y_f}}{\boldsymbol{\lambda_f}} \geq \frac{\boldsymbol{y_w}}{\boldsymbol{\lambda_w}} + \frac{\boldsymbol{1}}{\boldsymbol{h}} \quad (18)$$

which means that the contribution of the fouling deposit $R_f = \frac{y_f}{\lambda_f}$ ($m^2 \cdot K \cdot W^{-1}$) on the whole thermal resistance R_t ($m^2 \cdot K \cdot W^{-1}$) should be more important than those of the heat exchanger wall $R_w = \frac{y_w}{\lambda_w}$ ($m^2 \cdot K \cdot W^{-1}$) and the fluid convection $R_{convection} = \frac{1}{h}$ ($m^2 \cdot K \cdot W^{-1}$). This condition represents a critical value for the fouling thermal resistance, R_f, above which the fouling deposit can be detected by the FDP for a given configuration (wall thickness and conductivity) and operating condition (convection heat transfer coefficient, h).

In addition, the impact of the heat flux variation (between φ_0 and $\varphi_0+\Delta\varphi$) on the temperature difference measured by the probe is required to be significantly higher than that on the fluid temperature, i.e.:

$$\boldsymbol{\Delta T_p(y_f) \gg \overline{\Delta T_{FL}}} \quad (19)$$

In other words:

$$\boldsymbol{\overline{\Delta T_{FL}} = N \Delta T_p(y_f)} \quad (20)$$

inwhich $N < 1$. In our study, we consider N between 0.1 to 0.8 to be sure that the $\overline{\Delta T_{FL}}$is smaller enough than $\Delta T_p(y_f)$.

Taking into account equations (14) and (15), condition (20) can be rewritten as:

$$\boldsymbol{R_t \geq \frac{1 - N}{2N} \frac{S_p}{\dot{m} Cp}} \quad (21)$$

with: $R_t = \frac{y_w}{\lambda_w} + \frac{y_f}{\lambda_f} + \frac{1}{h}$

which helps to determine the critical value for the thermal resistance of the fouling deposit for a given flow rate and vice versa. The total thermal resistance should be greater than such a critical value in order that the FDP can detect the fouling thickness.

The FDP will be used in scenarios with and without fouling conditions. To ensure the statistical confidence, it is needed that the temperature difference measured by the probe in the two cases is higher than its uncertainty, meaning that:

$$\boldsymbol{\Delta T_p(y_f) - \Delta T_p(y_f = 0) \geq \delta T} \quad (22)$$

in which $\delta T = \pm 0.05°C$.

Combining equation (17) with condition (22) leads to:

$$\boldsymbol{\Delta \varphi \frac{y_f}{\lambda_f} \geq \delta T} \quad (23)$$

The heat flux applied to the FDP should fulfill condition (23) to ensure that the FDP is capable of detecting the fouling deposit.

The presented model provides a method to evaluate the fouling deposit thickness as a function of the induced temperature difference provided by the FDP (equation (17)) given the three required conditions (18), (21) and (23) which ensure statistical confidence of the results, are satisfied.

These conditions will be verified below for typical operating conditions found in food processing in which the FDP is located at the outer wall of the holder (simple tube located at the outlet of the tube-in-tube HX as illustrated in Fig. 2 and Fig. 3) to detect the fouling deposit formed at its inner wall (made of stainless steel). Table 2 summarizes the conditions and material properties required for the model.

Table 2. Conditions and material properties used in typical food processing.

Parameter	Value
Wall thickness, y_w [m]	0.001
Wall thermal conductivity, λ_w [$W \cdot m^{-1o} \cdot C^{-1}$]	20
Fouling conductivity, λ_f [$W \cdot m^{-1o} \cdot C^{-1}$]	0.67
Fouling thickness, y_f [m]	0.0005 to 0.002
FDP surface section, S_p [m^2]	$2.7e^{-4}$
Mass flow rate, $\dot{m}$[$kg \cdot h^{-1}$]	20~200
Heat capacity of working fluid, Cp [$J \cdot kg^{-1} \cdot °C^{-1}$]	4180
Convection heat transfer coefficient, h [$W \cdot m^{-2} \cdot K^{-1}$]	5~5000
Operating fluid temperature T_{FL} [°C]	80
Heat flux to be imposed, $\Delta\varphi$ [$W \cdot m^{-2}$]	5~100

Assuming that the fouling thickness varies between 0.5 to 2 mm, the calculation of criterion (21) shows a total thermal resistance R_t in the left hand side between 10^{-3} to 10^{-1} $m^2 \cdot K \cdot W^{-1}$ while the order of magnitude of the right hand side is 10^{-5} $m^2 \cdot K \cdot W^{-1}$ for N = 0.1 and 10^{-6} for N = 0.8 This means that under the conditions given in Tables 1 and 2, criterion (21) is always satisfied.

ISBN: 978-0-9984188-3-4; Published online www.heatexchanger-fouling.com

Fig. 6 and Fig. 7 determine the range of validation of criteria (18) and (23). It is noted that the critical values for the convection heat transfer coefficient h and for the heat flux $\Delta\varphi$ needed to be applied to the FDP are determined as the points where the criteria pass through zero (red dots in figs. 6 and 7). The calculation results shown in Fig. 6 give a critical value for the convection heat transfer coefficient, h, above which, the FDP is able to measure the thermal resistance of the fouling layer. As seen in Fig. 6, such critical values vary as a function of the detectable fouling thickness. For thick fouling layer, criterion is valid for low convection heat transfer coefficient. On the other hand, for a thin fouling deposit layer, high convection heat transfer is needed. Fig. 7 provides the required heat flux $\Delta\varphi$ to be applied to the FDP which is also dependent on the thickness of the fouling deposit layer

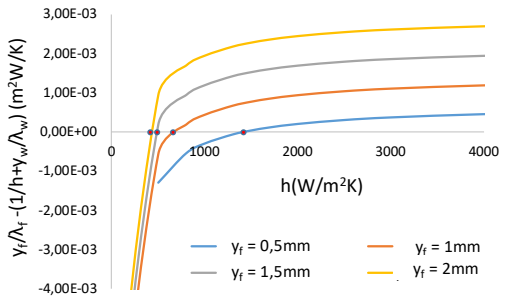

Fig. 6. Verification of condition (18) with the provided conditions in Table 1.

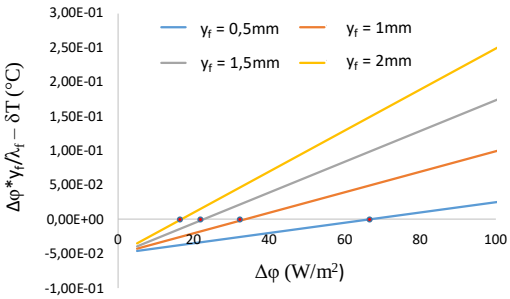

Fig. 7. Verification of condition (23) with the provided conditions in Table 1.

EXPERIMENTAL RESULTS

Fig. 8 shows the FDP signal during both thermal treatment and flushing steps.

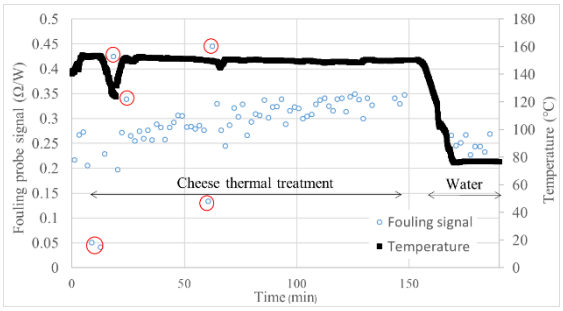

Fig. 8: FDP signal and temperature during a fouling and flushing test.

The FDP signal increases from 0.20 ± 0.010 to 0.35 ± 0.010 during the UHT treatment of the cheese-like fluid. The experimental measurements out of the main trend (dR_Ω/dP < 0.15 or > 0.4 $\Omega\cdot W^{-1}$) come from temperature gradients during the FDP measuring sequence. This means that these points are not relevant (red circles in Fig. 8). This experiment has been replicated and the fouling probe signal increases from 0.24 to 0.36 $\Omega\cdot W^{-1}$ (results not shown here).

The FDP signal increase is related to the fouling layer development. Around t = 150 min, rinsing water flows into the test rig, instead of cheese-like fluid, to start the cleaning procedure. Regarding the FDP signal, because of the change in flow convection conditions (change of fluid, change of fluid temperature, change of flowrate), the thermal environment of the FDP is different when the cleaning starts. Therefore, the values of the FDP signal before t =150 min and after t =150 min cannot be compared.

Fig. 9 illustrates the fouling layer that is observed at the end of the experimental test.

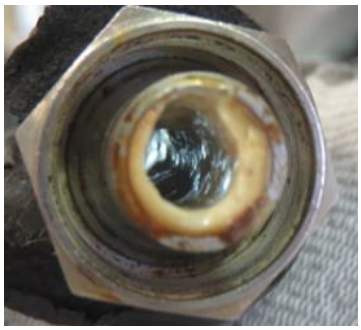

Fig. 9. Photograph of the fouling layer after water rinsing.

The FDP signal at the end of water rinsing is 0.25 ±0.015 $\Omega\cdot W^{-1}$. In similar flow conditions, but in a clean pipe, the signal measure is 0.18 ±0.010 $\Omega\cdot W^{-1}$. This is consistent with the appearance of a fouling layer as observed in Fig. 9.

Model validation

Fig. 8 provides the evolution of the FDP signal represented by dR_Ω/dP ($\Omega\cdot W^{-1}$). It is seen from Fig. 8 that during the cheese thermal treatment, the FDP signal dR_Ω/dP increases from 0.25 $\Omega\cdot W^{-1}$ (at the

ISBN: 978-0-9984188-3-4; Published online www.heatexchanger-fouling.com

beginning t = 0) to 0.35 $\Omega \cdot W^{-1}$ (at the end t = 150 min). In addition, at the end of the water rinsing, the measured FDP signal is 0.25 $\Omega \cdot W^{-1}$. For a clean pipe without any fouling deposit, this value is 0.18 $\Omega \cdot W^{-1}$ as above mentioned.

As described in the 1D model description, when the heat fluxes φ_0 and $\varphi_0+\Delta\varphi$ are applied to the FDP, the temperatures of the FDP are respectively denoted as $\boldsymbol{T'_p}$ and $\boldsymbol{T_p}$. Using equation (1), the corresponding electrical resistances of the probe are written as:

$$R_\Omega(T_p) = R_{\Omega,0}\left(1 + \alpha(T_p - T_0)\right) \quad (24)$$

and

$$R_\Omega(T'_p) = R_{\Omega,0}\left(1 + \alpha(T'_p - T_0)\right) \quad (25)$$

Hence, the difference between the two electrical resistances is:

$$\Delta R_\Omega = R_{\Omega,0}\alpha\Delta T_p \quad (26)$$

Combining equation (14), (15), (16) and (26) provides:

$$\Delta R_\Omega = R_{\Omega,0}\alpha\Delta\varphi R_t \quad (27)$$

This leads to:

$$\frac{\boldsymbol{dR_\Omega}}{\boldsymbol{dP}} = \frac{\boldsymbol{R_{\Omega,0}\alpha R_t}}{\boldsymbol{S_p}} \quad (28)$$

The left hand side of equation (28) represents the FDP signal. On the right hand side, α=0.00641°C^{-1} (for Nickel) and $R_{\Omega,0}$= 20.46 Ω.

The FDP signals obtained experimentally from Fig.8 are applied to equation (28) assuming that during each phase separately (fouling and cleaning), the convection and conduction (of the wall) thermal resistances did not vary. Also, the thermal conductivity of the fouling layer is assumed to be uniform as mentioned previously.

For the cheese thermal treatment phase:

- At t=0, $\frac{dR_\Omega}{dP} = 0.2$, then:

$$\frac{\boldsymbol{R_{\Omega,0}\alpha}}{\boldsymbol{S_p}}\boldsymbol{R_t}\Big|_{\boldsymbol{t=0}} \quad (29)$$

$$= \frac{\boldsymbol{R_{\Omega,0}\alpha}}{\boldsymbol{S_p}}\left(\boldsymbol{R_w + R_{convection,cheese}}\right) = \boldsymbol{0.2}$$

- With fouling, the FDP results in $\frac{dR_\Omega}{dP} = 0.35$, meaning that:

$$\frac{\boldsymbol{R_{\Omega,0}\alpha}}{\boldsymbol{S_p}}\boldsymbol{R_t}\Big|_{\boldsymbol{t=150}} \quad (30)$$

$$= \frac{\boldsymbol{R_{\Omega,0}\alpha}}{\boldsymbol{S_p}}\left(\boldsymbol{R_w + R_{convection,cheese} + R_{f,cheese}}\right) = \boldsymbol{0.35}$$

Combining equation (29) and equation (30) allows calculating the total thermal resistance R_t which takes into account the contribution of the heat exchanger wall conduction R_w, the fluid convection $R_{convection}$ and the fouling deposit conduction R_f. for cheese UHT treatment phase. Similar approach has been also applied for the water rinsing phase. As a result, the fouling thermal resistances are deduced as $1.44 \cdot 10^{-4}$ m$^2 \cdot$K$\cdot$W^{-1} for the water rinse phase and $3.08 \cdot 10^{-4}$ m^2 K$\cdot$W^{-1} for the cheese thermal treatment phase. One might say that during the water rinsing, a part of the fouling deposit formed during the cheese thermal treatment has been swept away. In addition, the convection heat transfer coefficients predicted from the FDP signals lead to 3100 W$\cdot$m$^{-2}\cdot$K^{-1} and 2800 W$\cdot$m$^{-2}\cdot$K^{-1} respectively for water rinse and cheese thermal treatment phases.

Alternatively, the heat convection coefficient, h, can be estimated using the following Dittus–Boelter equation:

$$\boldsymbol{Nu = 0.023 Re^{0.8} Pr^{0.33}} \quad (31)$$

Applying correlation (31) leads to $h_{water,correlation}$ = 3100 W$\cdot$m$^{-2}\cdot$K^{-1} and $h_{cheese,correlation}$ = 2100 W$\cdot$m$^{-2}\cdot$K^{-1}. While a good agreement has been obtained between value estimated by the correlation and the one deduced from experimental data of the FDP for water rinsing phase, a difference has been observed for the cheese thermal treatment phase. Such a difference might be explained by the following hypotheses:

- Firstly, the physical properties of the water are well-known but those of the cheese-like fluid are not;
- Second, the convective heat transfer coefficient is assumed to be constant from the beginning to the end of each phase (cheese UHT treatment and water rinsing) but it might not be the case in the reality due to the formation of the fouling layer and the resulting reduction of the hydraulic diameter.

Despite these assumptions, the order of magnitude is similar between the two values and, as a first step, it is sufficient to consider that the signals shown by the FDP are consistent with the development of the fouling deposit layer.

Using the thermal resistance of fouling layer as well as the thermal resistance of convection obtained above, the criteria (18), (21) and (23) of the 1D model could be checked for the cheese thermal treatment phase when the fouling deposit layer is formed. While criterion (21) is satisfied under current conditions, the criterion (23) is only validated for $\Delta\varphi$ > 200 W$\cdot$m^{-2} and the criterion (18) is met at high convective heat transfer coefficient (h > 3900 W$\cdot$m$^{-2}\cdot$K^{-1}). Under the currently considering conditions (h_{cheese} ~ 2100 W$\cdot$m$^{-2}\cdot$K^{-1} to 2800 W$\cdot$m$^{-2}\cdot$K^{-1}), the convection heat transfer is not strong enough, leading to important convective thermal resistance in comparison to the fouling one. However, as discussed previously, it is important to take into account the fact that several assumptions

ISBN: 978-0-9984188-3-4; Published online www.heatexchanger-fouling.com

have been made for thermal physical properties of the cheese-like fluid such as the thermal conductivity, the heat capacity, the viscosity, etc. which may result in potential calculation uncertainties. Therefore, further experiments with a known fluid with available physical properties should be carried out in the future in order to validate the criteria proposed by the 1D model and to confirm the feasibility of using the presented FDP for fouling detection.

CONCLUSION

This paper focuses on some theoretical aspects related to the use of a patented FDP for the determination of the local fouling status that comes along with thermal transfer across walls in fouling conditions. The local fouling status, the additional thermal resistance that comes along with fouling, as well as the margins to fouling development are determined by the presented FDP.

The measurement process relies on three main issues:

- Firstly, the capability to determine the local fouling thermal resistance from the FDP temperature;
- Secondly, the capability to handle both power release (heat flux) and temperature measurement within low uncertainty parameter ranges (eq.23) and without external flow perturbations.
- Lastly, the identification of the operating range under which the use of FDP for local fouling detection is reliable.

Each specific food process situation requires a careful analysis, utilizing specific geometrical configuration parameters, as well as, key operating conditions to determine whether the FDP is feasible/suitable for the considering application. Experimental results show that the FDP signal is consistent with the fouling layer development. The measured thermal resistances (convection and fouling) are consistent with prediction from both the model and the literature. This is the first validation step of this concept. The comparison of the FDP signal could be completed, in the future, with the monitoring of the heat input from the heating fluid used to maintain the outlet temperature of the product constant or with the monitoring of global metrics (pressure drop and HX thermal resistance). Also, the experimental set-up could be completed with two sandwiched FDPs to overcome limitations due to flow perturbation by measuring both the convection resistance and the fouling one. Future works should finally focus on the model validation with well-known fluids (unlike cheese-like fluid which is not fully characterized in terms of fluid properties) to avoid some assumptions. Also, a 2D model will be required to take into account the heat flux that flows into the pipe walls, especially when the fouling layer grows.

NOMENCLATURE

Cp Heat capacity of working fluid, $J \cdot kg \cdot °C^{-1}$
h Convection heat transfer coefficient, $W \cdot m^{-2} \cdot °C^{-1}$
$\dot{m}$ Mass flowrate of working fluid, $kg \cdot s^{-1}$
N Threshold value to be used in criterion (23)
Nu Nusselt number
P Power supplied for the FDP, W
Pr Prandtl number
R Thermal resistance, $m^2 \cdot °C \cdot W^{-1}$
Re Reynolds number
R_Ω Electrical resistance, Ω
$R_{\Omega,0}$ Electrical resistance at T_0, Ω
S_p Surface area of the FDP, m^2
T Temperature corresponding to the case when a heat flux φ_0 is applied to the FDP, °C
T' Temperature corresponding to the case when a heat flux $\varphi_0 + \Delta\varphi$ is applied to the FDP, °C
T_0 Reference temperature, °C
t Time, s
x Length, m
y Thickness, m
z Width, m
α Temperature coefficient of resistance, $°C^{-1}$
ΔT Temperature difference, °C
δT Uncertainty of temperature measurement, °C
$\Delta\varphi$ Heat flux increment applied to FDP, $W \cdot m^{-2}$
λ Thermal conductivity, $W \cdot m^{-1} \cdot °C^{-1}$
φ_0 Heat flux applied to the FDP, $W \cdot m^{-2}$

Subscript

f fouling
FL fluid
p probe
t total
w wall

REFERENCES

[1] H. U. Zettler, “Preface,” presented at the Heat Exchanger Fouling & Cleaning Conference, Józefów (Warsaw), Poland, Jun. 2019. [Online]. Available: https://heatexchanger-fouling.com/refereed-proceedings/heat-exchanger-fouling-and-cleaning-xiii-2019/

[2] B. Bansal and X. D. Chen, “A Critical Review of Milk Fouling in Heat Exchangers,” *Compr. Rev. Food Sci. Food Saf.*, vol. 5, no. 2, pp. 27–33, Apr. 2006, doi: 10.1111/j.1541-4337.2006.tb00080.x.

[3] E. Sadeghinezhad, S. N. Kazi, A. Badarudin, M. N. M. Zubair, B. L. Dehkordi, and C. S. Oon, “A review of milk fouling on heat exchanger surfaces,” *Rev. Chem. Eng.*, vol. 29, no. 3, Jan. 2013, doi: 10.1515/revce-2013-0003.

[4] P. Prasad, J. Gaffel, N. Price, and The Ecoefficiency Group Pty Ltd, “Eco-efficiency for the Dairy Processing Industry, 2019 Edition,” p. p.34, 2019.

ISBN: 978-0-9984188-3-4; Published online www.heatexchanger-fouling.com

[5] M. Ratel, Y. V. Kapoor, Z. Anxionnaz-Minvielle, L. Seminel, and B. Vinet, "INVESTIGATON OF FOULING RATES IN AN HEAT EXCHANGER USING AN INNOVATIVE FOULING RIG," in *Proceedings of International Conference on Heat Exchanger Fouling and Cleaning*, Budapest, Hungary: M.R. Malayeri, H. Müller-Steinhagen, A.P. Watkinson, Jun. 2013.

[6] L. Schnöing, W. Augustin, and S. Scholl, "Fouling mitigation in food processes by modification of heat transfer surfaces: A review," *Food Bioprod. Process.*, vol. 121, pp. 1–19, May 2020, doi: 10.1016/j.fbp.2020.01.013.

[7] E. Guelpa and V. Verda, "Automatic fouling detection in district heating substations: Methodology and tests," *Appl. Energy*, vol. 258, p. 114059, Jan. 2020, doi: 10.1016/j.apenergy.2019.114059.

[8] L. Perez, B. Ladevie, P. Tochon, and J. C. Batsale, "A new transient thermal fouling probe for cross flow tubular heat exchangers," *Int. J. Heat Mass Transf.*, vol. 52, no. 1–2, pp. 407–414, Jan. 2009, doi: 10.1016/j.ijheatmasstransfer.2008.05.029.

[9] L. Bouvier, G. Delaplace, and S. Lalot, "CONTINUOUS MONITORING OF WHEY PROTEIN FOULING USING A NON-INTRUSIVE SENSOR," in *Proceedings of International Conference on Heat Exchanger Fouling and Cleaning*, Aranjuez, Spain: M.R. Malayeri, H. Müller-Steinhagen, A.P. Watkinson, Jun. 2017.

[10] R. Guérin, G. Ronse, L. Bouvier, P. Debreyne, and G. Delaplace, "Structure and rate of growth of whey protein deposit from in situ electrical conductivity during fouling in a plate heat exchanger," *Chem. Eng. Sci.*, vol. 62, no. 7, pp. 1948–1957, Apr. 2007, doi: 10.1016/j.ces.2006.12.038.

[11] J. Escrig, E. Woolley, S. Rangappa, A. Simeone, and N. J. Watson, "Clean-in-place monitoring of different food fouling materials using ultrasonic measurements," *Food Control*, vol. 104, pp. 358–366, Oct. 2019, doi: 10.1016/j.foodcont.2019.05.013.

[12] E. Wallhäußer, M. A. Hussein, and T. Becker, "Detection methods of fouling in heat exchangers in the food industry," *Food Control*, vol. 27, no. 1, pp. 1–10, Sep. 2012, doi: 10.1016/j.foodcont.2012.02.033.

[13] X. D. Chen, D. X. Y. Li, S. X. Q. Lin, and N. Özkan, "On-line fouling/cleaning detection by measuring electric resistance—equipment development and application to milk fouling detection and chemical cleaning monitoring," *J. Food Eng.*, vol. 61, no. 2, pp. 181–189, Feb. 2004, doi: 10.1016/S0260-8774(03)00085-2.

[14] A. Simeone, B. Deng, N. Watson, and E. Woolley, "Enhanced Clean-In-Place Monitoring Using Ultraviolet Induced Fluorescence and Neural Networks," *Sensors*, vol. 18, no. 11, p. 3742, Nov. 2018, doi: 10.3390/s18113742.

[15] R. J. Hooper, W. R. Paterson, and D. I. Wilson, "Comparison of Whey Protein Model Foulants for Studying Cleaning of Milk Fouling Deposits," *Food Bioprod. Process.*, vol. 84, no. 4, pp. 329–337, Dec. 2006, doi: 10.1205/fbp06028.

[16] J. W. Choi *et al.*, "Temperature Difference-Based Fouling Detection in the Heat Exchanger of Gas-Solid Fluidized Beds," *Chem. Eng. Technol.*, vol. 45, no. 9, pp. 1623–1630, Sep. 2022, doi: 10.1002/ceat.202200188.

[17] Y. Boukazia *et al.*, "Metrological performances of fouling sensors based on steady thermal excitation applied to bioprocess," *Food Bioprod. Process.*, vol. 119, pp. 226–237, Jan. 2020, doi: 10.1016/j.fbp.2019.11.007.

[18] R. Murcek, J. Hölzel, H. Köhler, A. Boye, M. Hesse, and M. Mauermann, "Development of a quartz crystal sensor system to monitor local soil removal during cleaning in closed food processing lines," *Food Bioprod. Process.*, vol. 127, pp. 282–287, May 2021, doi: 10.1016/j.fbp.2021.03.011.

[19] D. I. Wilson, "Fouling during food processing – progress in tackling this inconvenient truth," *Curr. Opin. Food Sci.*, vol. 23, pp. 105–112, Oct. 2018, doi: 10.1016/j.cofs.2018.10.002.

[20] J. Veau, M. Petit, P. Tochon, and P. Clément, "Method and device for the detection and/or measurement of fouling in heat exchangers," WO 2009/153323, Dec. 23, 2009

[21] P. Tochon, P. Clément, and B. Ladevie, "Plate-type heat exhanger including a device for evaluating the extend to which it has become coated in scale," WO2007/099240, 2007

ISBN: 978-0-9984188-3-4; Published online www.heatexchanger-fouling.com